Induction of intrinsic apoptotic signaling pathway in A549 lung cancer cells using silver nanoparticles from *Gossypium hirsutum* and evaluation of *in vivo* toxicity

Nagarajan Kanipandian[a,b], Deyu Li[b], Soundarapandian Kannan[a,*]

[a] *Proteomics and Molecular Cell Physiology Laboratory, Department of Zoology, Periyar University, Salem, 636 011, TN, India*
[b] *Department of Hepato-Biliary Pancreatic Surgery, Henan Provincial People's Hospital, Zhengzhou, Henan Province, People's Republic of China*

A B S T R A C T

In the past decade, the research communities raised wide concerns on using medicinal plants for synthesis of nanomaterials due to its effective biological activity, lower side effects and also eco-friendly manner. Our previous report concentrated on the biomedical efficacy of fine characterized silver nanoparticles (AgNPs) from *Gossypium hirsutum* (cotton) leaf extract. Further, the current examination is planned to reveal the molecular mechanisms involving for activation of mitochondria-mediated signaling pathway by AgNPs in human lung cancer cells (A549) using various biological endpoints such as apoptotic induction by HOECHST 33342, AO/EtBr and Rhodamine 123 staining, cell cycle analysis using flow cytometry, gene and protein expressions by RT-PCR and immunoblotting respectively. This study was further extended to identify the toxicity of AgNPs using an animal model. Interestingly, we observed that A549 cells treated with AgNPs resulted in G_2/M arrest and ultimately leads to induction of apoptosis cell death. Moreover, gene analysis demonstrated that diminished expression of anti-apoptotic (Bcl-2) and enhanced expression of pro-apoptotic (Bax) mitochondrial genes. The alterations in the gene pattern may interrupt of mitochondrial membrane potential which facilitates the releasing of cytochrome c (cyt c) into cytosol. The cyt c act as a key molecule for activation of caspases (9 and 3) to initiate intrinsic apoptotic signaling cell death process. The histological analysis proven the application of AgNPs in nanomedicine is quietly harmless and would not cause any discernible stress like swelling and inflammation to the organs of mice. Taken together, this investigation may provide solid evidence for cotton crop mediated AgNPs induced apoptosis cell death pathway and offer a novel approach for cancer therapy.

1. Introduction

The utilization of nano-based materials for medical applications is called as nanomedicine, have led to the invention for the number of nanoparticles with enhanced peculiar features and multifunctional action such as disease diagnostics and treatment [1]. Among them, cancer nanotechnology comprises of science and engineering with broad applications for medicine such as molecular imaging, diagnosis of diseases, and targeted therapy [2]. In the past two decades, silver nanoparticle, especially from biological resources, is one of the most promising nanoproducts has been applied for nanomedicine due to its unique properties, broad spectrum and surface plasmon resonance effects. The major AgNPs characteristic features such as high conductive [3], optic [4] and biological properties [5] make them required for biological and engineering applications. The earlier report revealed that silver nanoparticles acted as an effective agent and showed its potential in biomedical applications [6].

The global scenario of lung cancer cell death is rapidly increasing because of long term adaptation of cancer-causing behaviors like smoking, physical inactivity and westernized diets

[7]. Among the various cancers, lung cancer is the leading cause of cancer death than any other cancers such as colorectal, breast and prostate cancers in developing countries [8]. Common treatments such as surgical procedures, radiotherapy, and chemotherapy approaches have been followed for cancer. Although, the existing conventional approaches are not successful [9,10] to increase the lifetime of cancer patients. Therefore, the available therapeutic procedures must be improved by novel techniques for early diagnosis and to target cancer, responsive signals for cell death with minimal side effects are instantly needed to enhance cancer therapy.

In this study, we used *Gossypium hirsutum* leaf extract as a substrate for AgNPs synthesis. The classification of *Gossypium hirsutum* comes under the family of Malvaceae, it's a perennial shrub and cultivated as annuals. Globally > 10 million farmers harvesting cotton and rely on the prospect for their income. The cotton is enriched of cellulose which is the natural fiber used for world textiles manufacture [11,12]. Our earlier reports described that there are fewer reports existing on biomedical applications but not with the anticancer investigation. Hence, we emphasized the anticancerous effect with distinct morphological changes in the A549 cells treated with AgNPs synthesized from cotton leaf extract [13]. Although, many kinds of literature available on anticancer activity of AgNPs but most of them are failed to address and quantify the expression of genes and proteins involved in the activation of the intrinsic apoptotic pathway. Hence, this investigation is mainly focused on revealing the molecular mechanism of mitochondrial-mediated apoptosis pathway in human lung cancer cells by AgNPs.

2. Materials and methods

2.1. Preparation of plant extract

The leaves of *Gossypium hirsutum* were collected and cleaned with double distilled water and shadow dried for 3 weeks. The leaves were made into powder form and 10 g of each powder extracted with 200 ml of methanol using Soxhlet apparatus for 14–16 h at solvent boiling temperature. Finally, the crude extract was collected and concentrated by rotary evaporator at 50 °C and stored at −20 °C until further use.

2.2. Gas chromatography linked mass spectrometric (GC–MS) analysis

A 100 μl of bis trimethylsilyl acetamide (BSTFA) was taken with 100 μl of plant extract, then 20 μl of pyridine was added. This solution was incubated for 1 h at 75 °C finally it was injected into GC–MS. The methanolic leaf extract of *Gossypium hirsutum* was quantitatively performed by GC-170 MS (Shimadzu QP 2010 PLUS system, Japan) equipped with a capillary column (30 m × 0.25 mm i.d. × 0.25 μm film thickness). Splitless injection was performed with a purge time of 1 min. The carrier gas was helium at a flow rate of 1 ml/min. The column temperature was retained at 50 °C for 3 min, then programmed at 5 °C/min to 80 °C and then at 10 °C/min to 340 °C. The inlet temperature was 280 °C, the detector temperature was 360 °C and the solvent delay was 4 min. The identification of the peaks was based on computer matching of the mass spectra with WILLY.8 LIB library and by direct comparison with published data.
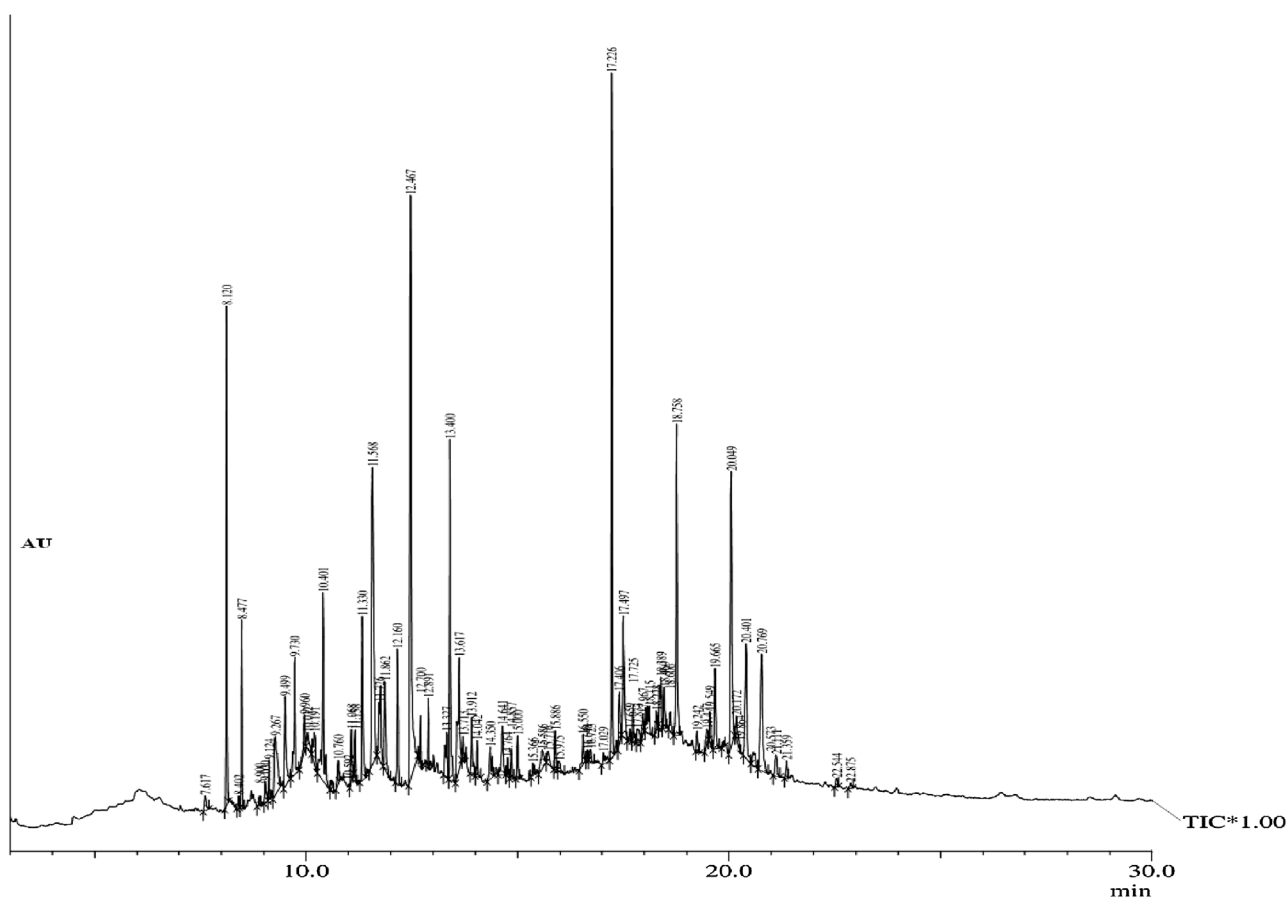

Fig. 1. GC–MS Chromatogram for methanol leaf extract of *G. hirsutum*.

Table 1

Characterization of AgNPs synthesized from aqueous leaf extract of *Gossypium hirsutum.*

Methods used for Characterization	Observation
UV-visible spectroscopy	410 nm
FTIR	Presence of proteins, phenolic compounds and silicon (Si-O-Si) may act as a reducing agent to form Ag ions
XRD	Face centered cubic structure (JCPDS File No: 03-0921) and crystalline nature with 13 nm size
EDX	Elemental constituents of silver (64.88 %), carbon (14.69 %), Chloride (10.29 %), oxygen (9 %) and calcium (1.14 %)
FESEM and HRTEM	Mono-dispersed nature and spherical in shape with size range between 13 to 40 nm
SAED	Confirm the crystalline nature of the silver nanoparticles

2.3. Synthesis and characterization of AgNPs

The AgNPs was synthesized by mixing of leave extract and 1 mM silver nitrate (HIMEDIA) solution and the color change was observed. The prepared AgNPs undergone to investigate the characteristic features performed by UV–Vis spectra showed the maximum absorbance at 410 nm and Fourier transform infrared spectroscopy (FTIR) confirmed the presence of proteins, phenolic compounds and silicon (Si-O-Si) may act as a reducing agent to form Ag ions. The X-ray diffraction (XRD) demonstrated a face-centered cubic structure (JCPDS File No: 03-0921) and crystalline nature with 13 nm size. The scanning electron microscopy (SEM) and transmission electron microscopy (TEM) were revealed mono-dispersed nature and spherical in shape with a size range between 13–40 nm [13]. Additionally, the dynamic light scattering technique was done with Zetasizer Nano-ZS (Malvern Instruments Ltd., Malvern, UK).

2.4. A549 cell culture maintenance and IC_{50} concentration

The A549 cells were cultured in Dulbecco's Modified Eagles Medium (DMEM) with required nutritional supplementation and minimal inhibitory concentration of AgNPs was about 40 μg/mL using MTT assay and it is previously reported [13]. Hence, we extended the current examinations by following the above mentioned IC_{50} concentration to report the cell death signaling pathways.

2.5. HOECHST 33342 staining for nuclear apoptosis

The A549 lung cancer cells were maintained in 6 well plates and treated with AgNPs using IC_{50} concentration for various time duration like 24, 48 and 72 h. At each time point, the cells were washed twice with PBS, harvested by trypsinization. Then the cells were fixed in 4% paraformaldehyde for 20 min and re-washed, finally stained with HOECHST 33342 (10 μg/mL) at 37 °C for 20 min in the dark [14]. The surplus stains were removed by washing with methanol followed by PBS, and plates were then focused for determining any nuclear structural changes and apoptotic bodies caused by AgNPs under blue channel fluorescence with fluorescent microscopy (Nikon Eclipse, Inc., Japan).

2.6. Direct fluorescence microscopic analysis for apoptosis induction

Acridine orange/ethidium bromide (AO/EB) staining procedure was followed out to detect the morphological indication of
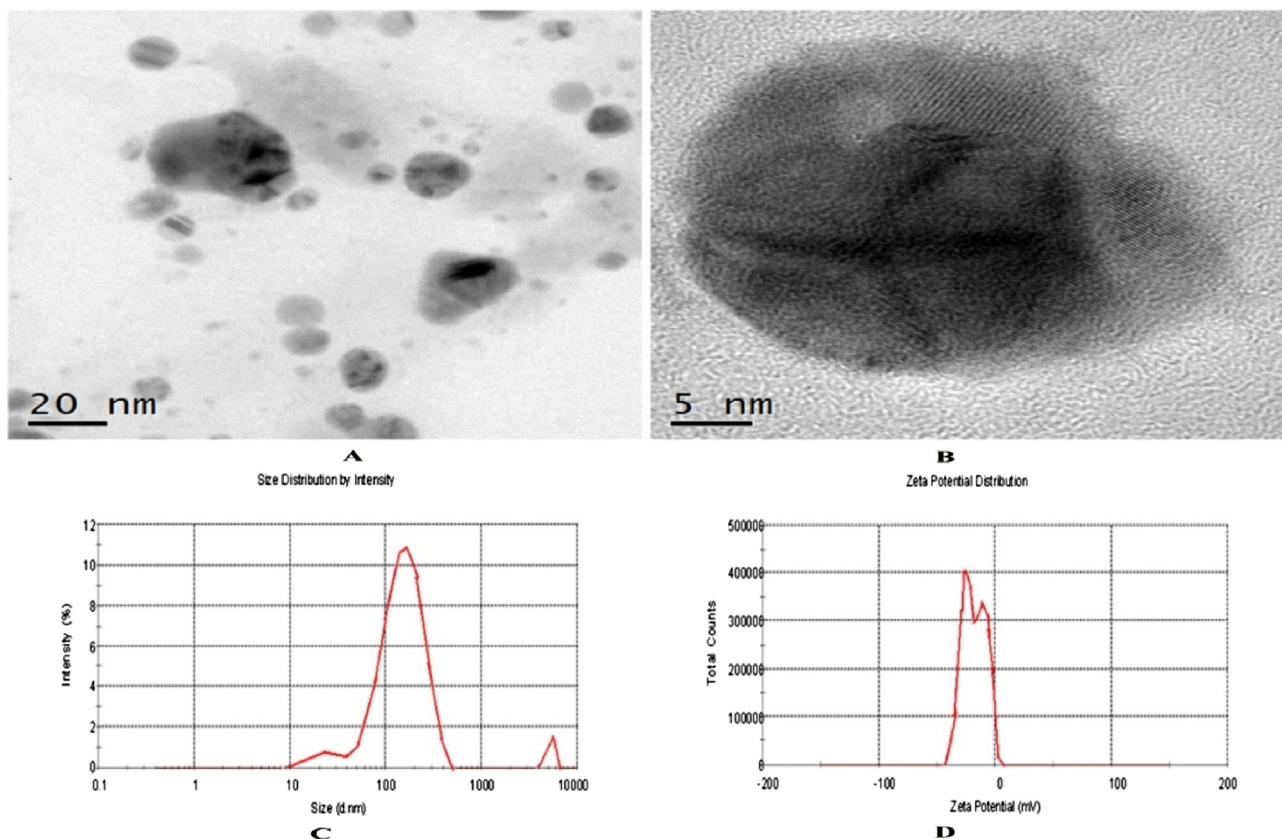

Fig. 2. Represents the HRTEM (A) Size (B) and Zeta potential of cotton leaf mediated AgNPs.

Table 2
Profiling chemical constituents of *G. hirsutum* through GC–MS analysis.

Peak#	R. Time	Area	Area%	Name
1	7.617	583955	0.30	8-ISOPROPYL-1,3-DIMETHYLTRICYCLO[4.4.0.02,7]
2	8.120	11884797	6.07	Caryophyllene
3	8.402	368270	0.19	5,9-UNDECADIEN-2-ONE,6,10-DIMETHYL-,(E)-
4	8.477	4251320	2.17	1,4,8-CYCLOUNDECATRIENE,2,6,6,9-TETRAMETHYL-
5	8.900	272285	0.14	
6	9.030	672980	0.34	Bicyclo[3.1.1]hept-2-ene,2,6-dimethyl-6-(4-methyl-3-penteny
7	9.124	874454	0.45	.beta.-Bisabolene
8	9.267	4078334	2.08	D-Allose
9	9.499	3215656	1.64	Dodecanoicacid
10	9.730	3777187	1.93	Caryophylleneoxide
11	9.960	1151273	0.59	
12	10.032	853161	0.44	.alpha.-ᴅ-Galactopyranoside,methyl
13	10.191	1765188	0.90	Caryophylleneoxide
14	10.401	6539998	3.34	.beta.-bisabolol
15	10.592	479959	0.25	3-Buten-2-one,4-(4-hydroxy-2,2,6-trimethyl-7-oxabicyclo[4.1
16	10.760	793106	0.41	2-Cyclohexen-1-one,4-(3-hydroxybutyl)-3,5,5-trimethyl-
17	11.068	1504771	0.77	Tetradecanoicacid
18	11.158	978029	0.50	MYRACALDEHYDE1AND2
19	11.330	5070493	2.59	3-Buten-2-ol,2-methyl-4-(1,3,3-trimethyl-7-oxabicyclo[4.1.0]
20	11.568	13840588	7.07	2,6,10-TRIMETHYL,14-ETHYLENE-14-PENTADECNE
21	11.726	3423698	1.75	
22	11.862	3166693	1.62	2-HEXADECEN-1-OL,3,7,11,15-TETRAMETHYL-,[R-[R
23	12.160	3256937	1.66	Hexadecanoicacid,methylester
24	12.467	20632200	10.54	n-Hexadecanoicacid
25	12.700	1020294	0.52	2,6,10-Dodecatrien-1-ol,3,7,11-trimethyl-
26	12.891	1309589	0.67	GERANYLLINALOOLISOMER
27	13.327	1939100	0.99	9,12,15-Octadecatrienoicacid,methylester,(Z,Z,Z)-
28	13.400	8593632	4.39	Phytol
29	13.617	5352556	2.73	9,12,15-Octadecatrienoicacid,(Z,Z,Z)-
30	13.713	605854	0.31	Octadecanoicacid
31	13.912	1725351	0.88	Hexadeca-2,6,10,14-tetraen-1-ol,3,7,11,16-tetramethyl-
32	14.042	815734	0.42	4,5,6,7-TETRAETHYL-1-METHYLINDANE
33	14.350	1473472	0.75	2,6,10-Dodecatrien-1-ol,12-acetoxy-2,6,10-trimethyl-,(E,E,E
34	14.641	1948533	1.00	cis-9-Hexadecenal
35	14.764	444061	0.23	Cyclohexane,tetradecyl-
36	14.857	681232	0.35	4,8,12,16-Tetramethylheptadecan-4-olide
37	15.000	938872	0.48	5,9,13-Pentadecatrien-2-one,6,10,14-trimethyl-,(E,E)-
38	15.366	303529	0.16	1,6,10,14,18,22-Tetracosahexaen-3-ol,2,6,10,15,19,23-hexa
39	15.586	1396225	0.71	Hexadecanoicacid,trimethylsilylester
40	15.716	640220	0.33	Hexadecanoicacid,2-hydroxy-1-(hydroxymethyl)ethylester
41	15.886	923212	0.47	Bis(2-ethylhexyl)phthalate
42	15.975	473608	0.24	CYCLOHEXANONE,2,6-BIS(PHENYLMETHYLENE)-
43	16.550	1011252	0.52	2-methylhexacosane
44	16.648	237719	0.12	9,19-Cyclolanostan-3-ol,acetate,(3.beta.)-
45	16.723	329362	0.17	Formicacid,3,7,11-trimethyl-1,6,10-dodecatrien-3-ylester
46	17.029	681555	0.35	2-methylhexacosane
47	17.226	15110297	7.72	Squalene
48	17.406	1789642	0.91	Cyclohexane,1,2,3,5-tetraisopropyl-
49	17.497	4339880	2.22	Tetratetracontane
50	17.659	412950	0.21	
51	17.725	948319	0.48	NERYLLINALOOLISOMER
52	17.833	858417	0.44	
53	17.967	814440	0.42	PENTALENE,OCTAHYDRO-1-(2-OCTYLDECYL)-
54	18.115	1743851	0.89	1,6,10,14,18,22-Tetracosahexaen-3-ol,2,6,10,15,19,23-hexa
55	18.278	471811	0.24	.beta.-Tocopherol
56	18.389	2138161	1.09	Tetratetracontane
57	18.460	1308405	0.67	1-Triacontanol
58	18.606	605150	0.31	Cholesta-4,6-dien-3-ol,(3.beta.)-
59	18.758	8832148	4.51	Vitamin E
60	19.242	529283	0.27	SOLANESOL
61	19.477	759746	0.39	
62	19.549	865411	0.44	1-Heptacosanol
63	19.665	2761176	1.41	Stigmasterol
64	19.864	170541	0.09	ARNOTHIANAMIDE
65	20.049	10258322	5.24	STIGMAST-5-EN-3-OL,(3.BETA.)-
66	20.172	989293	0.51	Fucosterol
67	20.401	4643699	2.37	.beta.-Amyrin
68	20.573	919433	0.47	4,4,6A,6B,8A,11,11,14B-OCTAMETHYL-1,4,4A,5,6,6A,6
69	20.769	5978914	3.05	.alpha.-Amyrin
70	21.111	1001969	0.51	Cholest-4-en-3-ol
71	21.359	574185	0.29	Phytol,acetate
72	22.544	351682	0.18	SOLANESOL
73	22.875	252974	0.13	2,2,4-Trimethyl-3-(3,8,12,16-tetramethyl-heptadeca-3,7,11,15
		195710393	100.00	

apoptosis on the AgNPs treated cells [15]. The cells were fixed in 3:1 ratio of methanol and glacial acetic acid for 1 h at room temperature. The cells treated with AgNPs (24, 48 and 72 h) were labeled with 1:1 ratio of AO and EB in PBS and incubated for 5 min then the excess unbinding dye was removed by washing with PBS. Stained cells were visualized under using fluorescence microscope (Nikon Eclipse, Inc., Japan) at 100× magnification with an excitation filter at 480 nm.

2.7. Rhodamine 123 staining

Modifications in mitochondrial membrane constancy as an effect of treating with AgNPs were measured by Rhodamine-123 staining [16]. The A549 cells were seeded in 6 well plates (1×10^5 cells/well) and exposed to AgNPs. After the 24, 48 and 72 h treatment, the cells were collected and fixed in 4% paraformaldehyde. After hard fixing, the cells were washed twice with PBS and stained with Rh-123 (10 μg/mL) for 30 min at 37 °C. Further, extra stains were removed by methanol and again washed with PBS. The cells were analyzed for alteration in Δψm using fluorescence microscope with an excitation and emission wavelengths of 505 nm and 534 nm, respectively.

2.8. Cell cycle analysis

The cell cycle arrest was investigated by the modified protocol of Thangam et al., [17]. The cells (1×10^6) were cultured in a tissue culture dish and keep them to mature all-night. The cells were treated for 72 h and cells without AgNPs kept as control. After attained at 75% of confluence, the cells were trypsinized and collected in appropriate centrifuge tubes. Then centrifuged at 2500 rpm for 5 min at RT (room temperature) and cells in the pellet were re-suspended in 300 μL of PBS–EDTA to which 700 μL of chilled 70% ethanol was added drop-wise with slow mixing. The solution

was added to assure absolute combination of ethanol, and the samples were stored at 0 °C overnight. Subsequently, 1:100 volumes of 20 mg/mL RNase were added to remove RNA contamination, and the mixture was incubated at 37 °C for 1 h. Propidium iodide was added to a final concentration of 50 μg/mL and incubated for 10–20 min at room temperature in dark. The stained cells were analyzed for DNA histograms and for cell cycle phase distribution using flow cytometry (Becton Dickinson Immuno cytometry System, USA)

2.9. Semi-quantitative RT-PCR analysis for apoptotic gene expression

The changes in the expression profile of Bax, Bcl-2, p53 and β-Actin genes were identified using RT-PCR analysis. For this study, TriZol reagent was used to separate the total RNA from AgNPs treated A549 cells. Briefly, the cDNA was synthesized using a cDNA synthesis kit and amplified accordant to the manufacturers protocols in a 25 μL of reaction mixture included random primer pairs (1.0 μL): 10× buffer (5.0 μL), cDNA (2.0 μg), 25 mM/L MgCl (3.0 μL), 10 mM/L dNTPs (1.0 μL), and Taq polymerase (2.5 U). Semi-quantitative RT-PCR amplification cycles have denaturation at 94 °C for 1 min, primer annealing at 57 °C for 45 s and extension at 72 °C for 45 s, for a total of 30 cycles followed by terminal extension at 72 °C for 10 min. The primer sequences are followed according to Thangam et al., [17].

2.10. Western blotting analysis

Western blotting was executed [18] to observe the expression of apoptosis accountable proteins such as cytochrome c, caspase 9 and caspases 3 in A549 cells. The cells (2×10^6) were seeded onto 100-mm culture dishes in the presence or absence of AgNPs. After 20 min, the lysates were centrifuged at 12,000 rpm for 10 min at 4 °C and supernatants were stored at −80 °C until further use. Proteins (30 μg/lane) were separated using 10% SDS-PAGE and
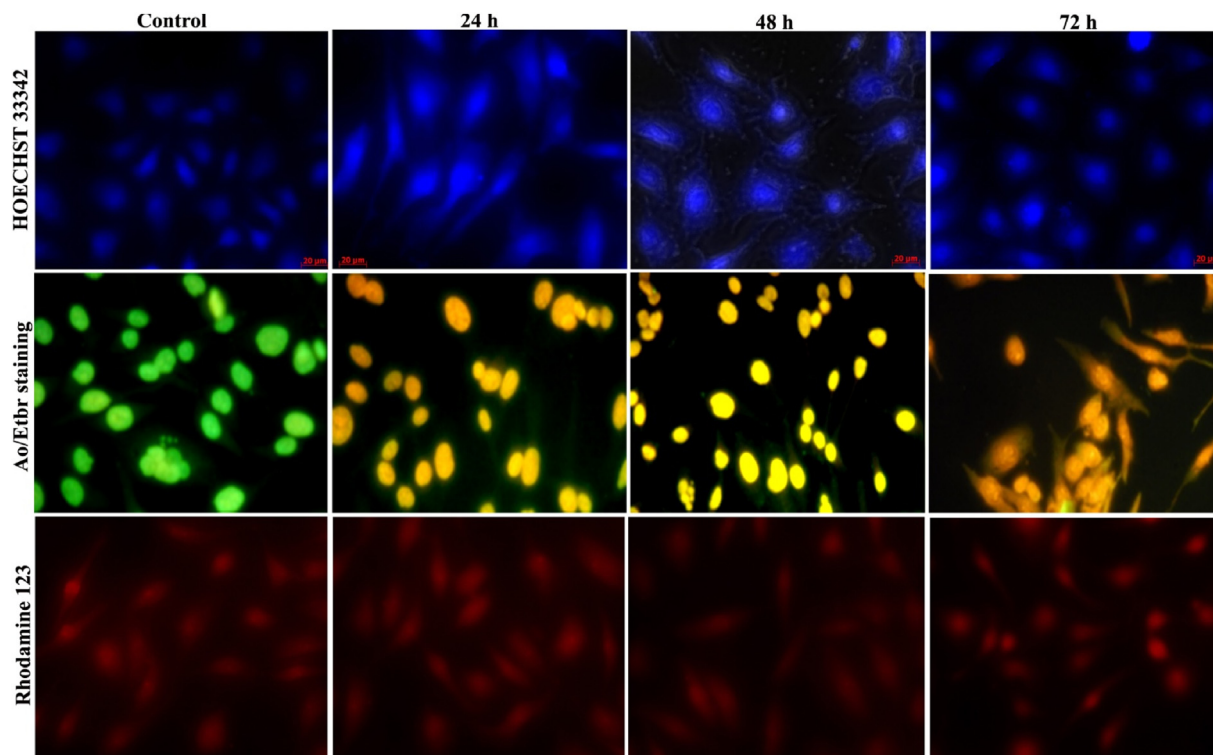

Fig. 3. Fluorescence microscopy images of control and silver nanoparticles treated A549 cells. The apoptosis induction by HOECHST-33342, AO/EtBr staining and loss of mitochondrial membrane potential by Rh-123 staining at different time intervals (24, 48 and 72 h).

then transferred to PVDF membrane. Afterward, the membranes were blocked in TBST solution containing 5% (w/v) non-fat milk for 2 h, followed by overnight incubation at 4 °C with primary antibodies such as caspase 9 and 3, cytochrome c and β-actin. After being washed with TBST buffer, the membranes were incubated for 1 h with the secondary antibody, horseradish peroxidase-conjugated goat anti-rabbit IgG. Antibody-bound proteins were detected using enhanced chemiluminescence reagents. Blots were washed with washing buffer and incubated with secondary antibodies conjugated with horseradish peroxidase for 1 h at room temperature.

2.11. In vivo histopathological study

To assess the non-toxic effect of AgNPs, the present research was promoted for histopathology analysis [6]. Male Balb-c mice (aged 6 weeks, 18 ± 2 g) were acquired from King Institute of Preventive Medicine, Chennai and maintained under standardized-environmental situation at the ambient temperature of 25 °C. Animals were preserved with humanly healthy care and supplied with food and water ad libitum. A total of 12 mice were distributed into two groups. One group was treated with AgNPs (40 μg/mL) and second as control

group having 200 μL saline were intravenously administrated for every 4 days (day 1, day 5, and day 9) through tail veins. The body weight was enrolled for the entire experiment. On the 12th day, the coefficients of liver, heart, kidneys, brain, spleen, testis and lung and to body weight were measured as the ratio of tissues (wet weight/mg) to body weight (g). The major tissues were dissected and were fixed in 10% formalin, embedded in paraffin, sectioned and stained with hematoxylin and eosin (H&E) for the histological test using standard techniques. After staining, images were taken using an optical microscope.

2.12. Statistical analysis

All the experiments were carried out in triplicates and the data were expressed as mean ± SEM. The difference between means was analyzed by one-way ANOVA. All statistical analyses were performed using SPSS 17.0 software. A level of $p \leq 0.05$, $p \leq 0.01$ was taken as statistically significant.

3. Results and discussion

The GC–MS study was carried out in Gossypium hirsutum leaf extract, it displayed 73 peaks (Fig. 1) and the leading peaks such as
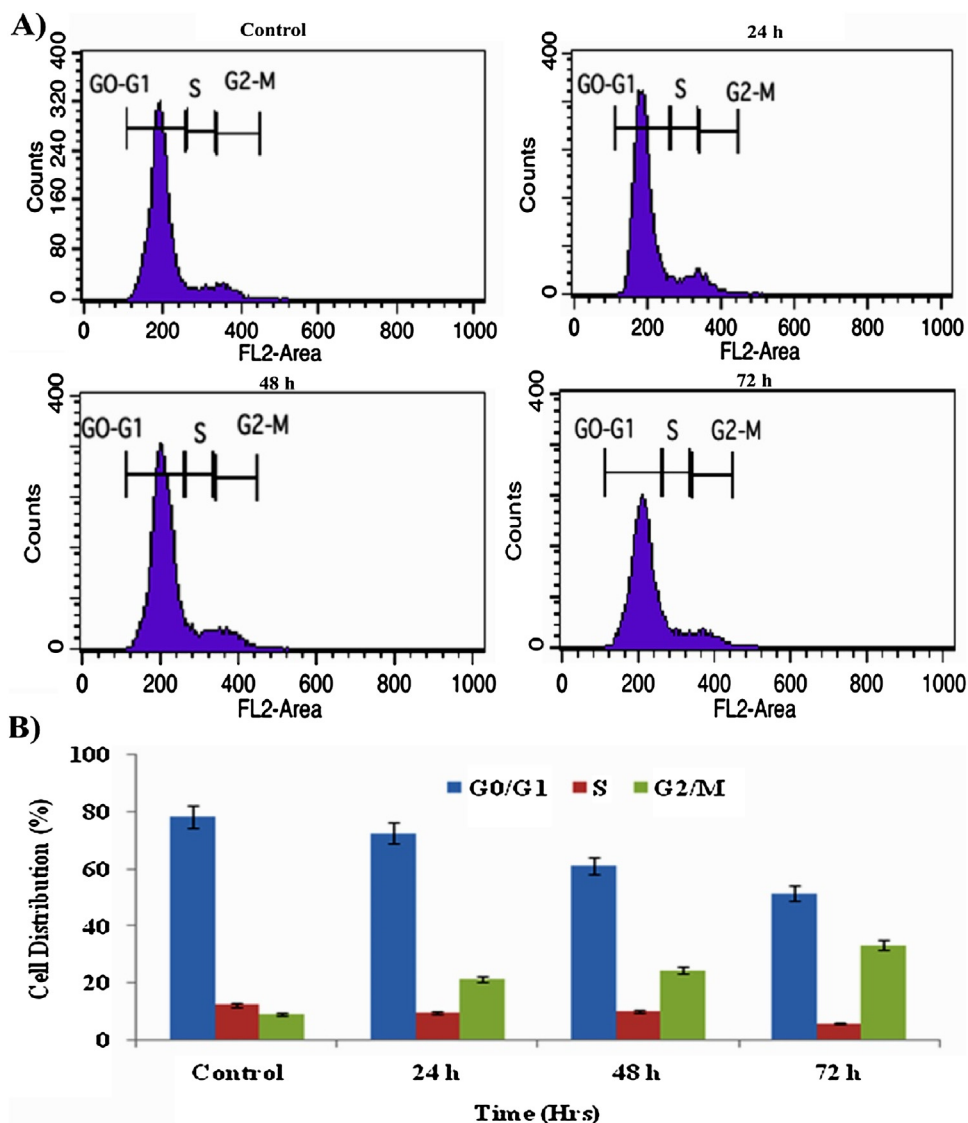

Fig. 4. (A) Flow cytometric analysis of cell cycle distribution of AgNPs treated and control A549 cells for 24, 48 and 72 h (B) depicts the cellular DNA histograms of A549 cells were analyzed by the BD CELLQuest Pro.

Caryophyllene (6.07%), 2, 6, 10-Trimethyl, 14 ethylene-14-penta-decne (7.07%), n-Hexadecanoic acid (10.54%), Phytol (4.39%), Squalene (7.71%) and Vitamin E (4.51%) were perceived in higher composition (Table 1).

The AgNPs were well characterized using the different methods. The HRTEM images are presented in Fig. 2 A and B which evidenced spherical construction of the particles. The mean size of the AgNPs was between 23.5–163.7 nm calculated by DLS. ZP quantity determined in this study is −18 mV (Fig. 2C and D) and it showed the superficial charge and stability of the particles (Table 2)

3.1. HOECHST 33342 staining for nuclear apoptosis

In this study, the execution of apoptosis was explored by staining lung cancer cells treated with IC_{50} property of biogenic AgNPs with HOECHST 33342. It is previously proven that HOECHST 33342 stain is cell-permeable and well adhered to the adenine-thymine rich domain of the minor groove of DNA. This is comprehensively exploited to stain DNA to assess the cell cycle, apoptosis, and measure viable cells by flow cytometry [19]. Interestingly, evidential modification for apoptosis inductance was discovered between the control and treated cancer cells with AgNPs for 24 h, 48 h and 72 h (Fig. 3). The control cells had an integral round typical nucleus with orderly morphology released a debilitated blue fluorescence by HOECHST 33342 stains. Whereas, the AgNPs treated cells displayed aglow blue color emission of apoptotic nuclei which were acknowledged by condensed and disunited nuclei and chromatin collected at the boundary of the nuclear membrane. Besides, it noticed that the induction of

apoptosis was enhanced in AgNPs treated cells. This examination distinctly pointed with cell growth retardation was evoked by AgNPs. A previous study of Sharma et al. [14] analyzed the analogous effects like DNA contraction and the apoptotic dead body in zinc oxide nanoparticles treated human liver cells (HepG2).

3.2. Study of apoptosis induction by AO/EtBr

Apoptosis can be activated by changes in membrane unity, suppression of cell development, cytoplasmic contraction, and cell clumping [14]. In existing research, the apoptotic cells were distinguished from one another using fluorescence microscopy. The apoptotic cells containing dead bodies were ascertained as orange colored whereas the necrotic cells emitted a red color. The control A549 cells were expelled consistent green fluorescence color which pointed cells are live. After treatment with AgNPs for 72 h, the cells were determined with defined morphological modification such as the contrasting dimension of nuclear morphology during apoptosis, condensed nuclei, membrane, blebbing and apoptotic fragments (Fig. 3).

3.3. Analysis of mitochondrial membrane potential ($\Delta \psi m$) by Rh-123 staining

The potentiality of mitochondrial membrane acts a crucial constituent for induction of apoptotic activity of cell death. Therefore, we have proven the mitochondrial membrane stability of A549 cells using Rh-123 dye for 24, 48 and 72 h AgNPs treatment. The fluorescence representation (Fig. 3) of current examination distinctly showed the loss of $\Delta \psi m$ owed to
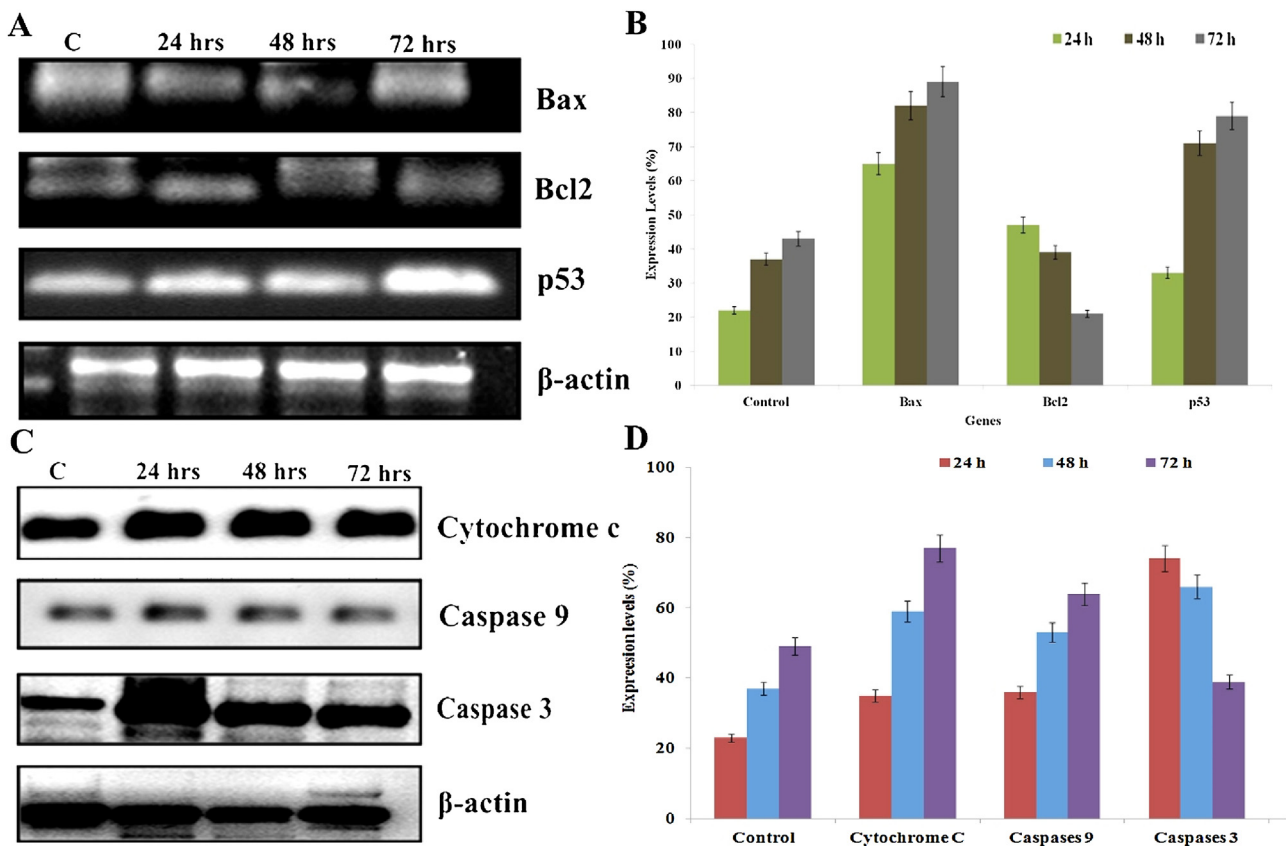

Fig. 5. (A) The semi-quantitative RT-PCR demonstrates the gene expression changes for Bax, Bcl-2, p53 and β-actin (B) Densitometry analysis of intrinsic apoptotic related gene expressions of A549 cells exposure to AgNPs for 24, 48 and 72 h. The results shown here are representative of three independent experiments. (C) Immunoblot showing the expression of apoptotic responsive proteins such as cyt c, caspases -9, caspases -3 and β-actin (D) Densitometry quantification of apoptotic protein expression. The results exhibited here are representative of three independent experiments. β-actin expression was used as a loading control.

mitochondrial membrane depolarization and besides observed that fluorescence strength was attenuated with accelerating the exposure time of AgNPs. The corresponding effect was observed by Siddiqui et al. [20] that decreased fluorescent intensity indicate the significant reduction of mitochondrial membrane stability in human hepatocarcinoma cells (HepG2) treated with CuO NPs. Also declared that loss of mitochondrial membrane integrity of the cancer cells by depolarization and dysfunction leads to cell death [16]. A previous report of McBride et al. [21] agreed that mitochondria are participating in major function such as signaling, cellular differentiation, cell death, control of cell cycle and cell growth. It is likewise expressed that interruption and regulation of permeability of mitochondrial outer membrane lead to the stimulation of cascade of caspases by the effect of some apoptotic stimuli [22–24]. The overall findings strengthen that AgNPs activated the intrinsic apoptotic signaling pathway result by biochemical and physiological alterations in the A549.

3.4. Effects of AgNPs on cell cycle regulation

The goal of this study is to examine the distribution of AgNPs treated cells in various phases of the cell cycle by flow cytometry.

The treatment of A549 cells with AgNPs (IC_{50} concentrations) for several periods of time (24, 48 and 72 h) resulted in a decrease of the G_2/M phase comparison with the control. The data of flow cytometry study showed AgNPs treatment in A549 cells arrested in the G_2/M phase of the cell cycle with time-dependent manner (Fig. 4). The effect of AgNPs in arresting the A549 cells in G_2/M form of the cell cycle convey the existence that cotton leaf extract mediated AgNPs may also be useful for the control of cancer cell growth. The related effect was observed on selenium nanoparticles induced cell cycle arrest in A549 cells [25].

3.5. Effect on apoptotic gene and protein expression analysis

This investigation exhibits the mechanism implicit AgNPs mediated mitochondria-dependent apoptotic cell death triggered in A549 cells. The gene expression of both anti-apoptotic and apoptotic at protein level of AgNPs exposed lung cancer cell was analyzed using semi-quantitative RT-PCR and Western blot technique. The cells were treated with IC_{50} concentration of AgNPs for 24, 48 and 72 h. At each time point, total apoptotic (Bax) and anti-apoptotic genes (Bcl-2) and proteins (cytochrome c, caspase -9 and caspase -3) were isolated, and expression levels
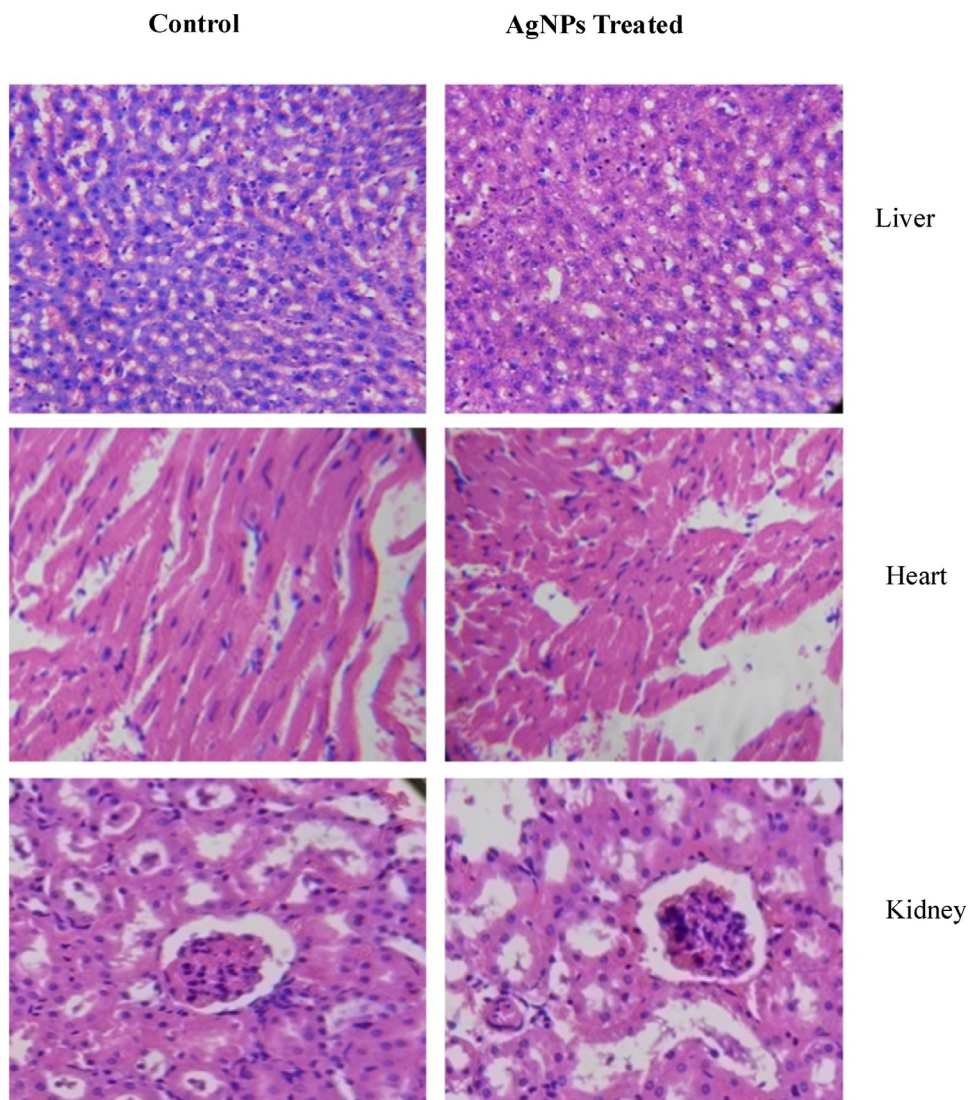

Fig. 6. *In vivo* toxicity investigation of AgNPs on mice organs such as liver, heart and kidney. The control group images are given in A, C and E and AgNPs treated images are in B, D and F.
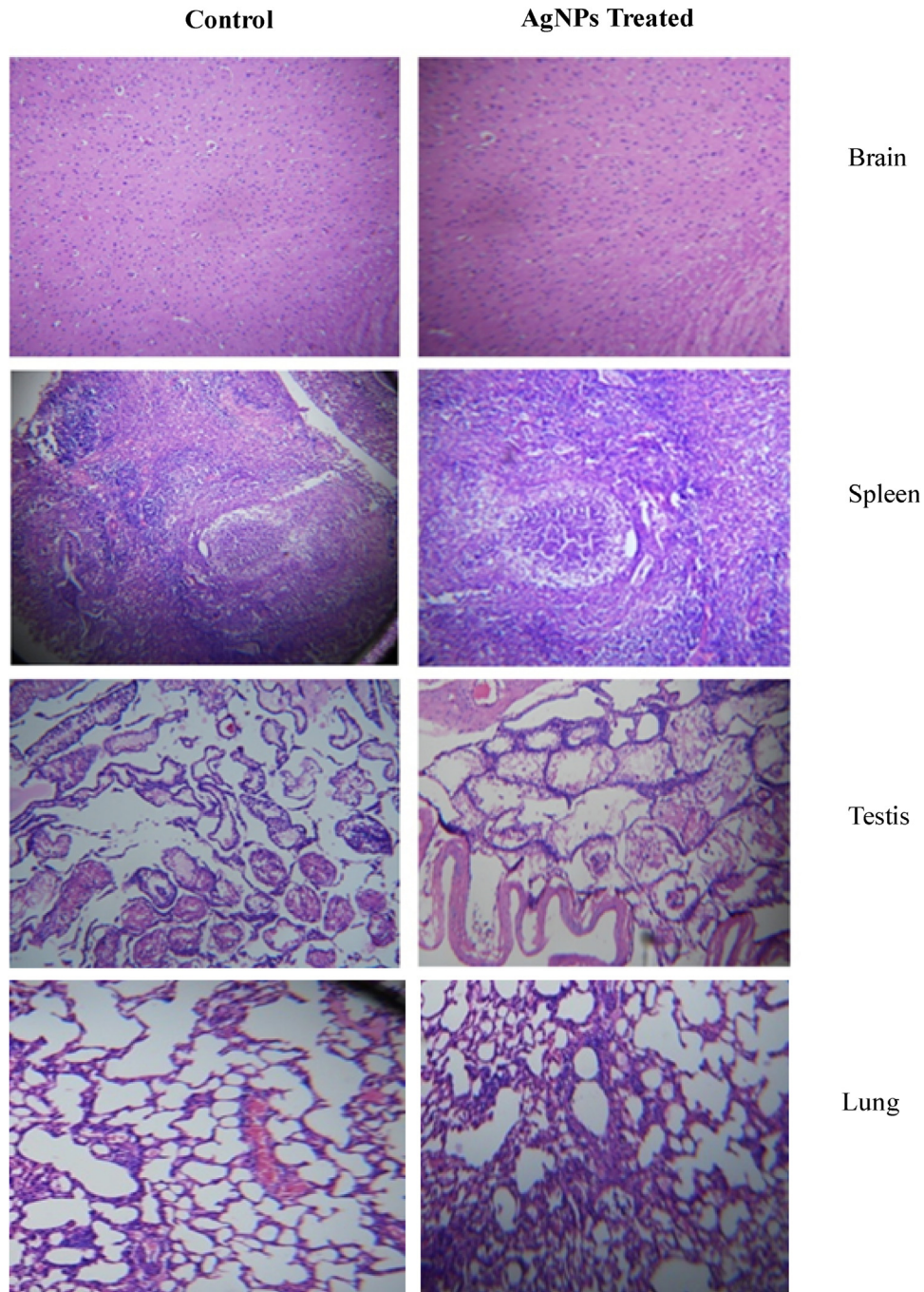
Fig. 7. Depict the histopathological observations of control and AgNPs treated group of mice. The histological analysis of brain, spleen, testis and lung demonstrate there is no significant difference between the control (A, C and E) and AgNPs treated (B, D and F) groups. This proves the insignificant toxicity of silver nanoparticles against the selected vital organs.

were calculated by RT-PCR and Western blot analysis. The current examination was aimed at the expression level of Bax, Bcl-2 and p53 genes and it displayed an evidential that Bcl-2 expression was suppressed and excitingly up-regulated expression of Bax and p53 in AgNPs treated cancer cells when compared with control cells. It has been proven that the enhanced expression of Bax represents the key effector of the intrinsic pathway liable for the induction of mitochondrial modifications [26]. The time-dependent activity was observed, which showed up-regulated the expression of genes/protein with increased time of exposure to AgNPs (Fig. 5). The decreased Bcl-2 level indicate that AgNPs effectively inter-mediated the intrinsic apoptotic activity by inhibiting the anti-

apoptotic gene expression. An earlier report evidenced Bax showed a fundamental function in the inhibition of the anti-apoptotic role of Bcl-2. The overexpression of Bcl-2 level leads to suppression of cytochrome c release from the mitochondria to the cytoplasm and block the caspase activation step of the mitochondrial mediated-intrinsic apoptotic pathway [27,28].

The current investigation also addressed the expression of p53 in the treated cells and it was observed that the level of p53 expression increased dramatically in time-dependent manner. From this measurement, the present study confirmed that the up-regulation of the p53 act as a primal role in the activation of the apoptosis process. It has been investigated earlier that apoptotic signaling

mediated by p53 generate amino terminal conformational alteration which evidence to release of cytochrome c from mitochondria. The cytochrome c facilitates the cleavage of caspases -9 and -3 and eventually apoptosis cell death has taken place [17,29]. In this study, the β-actin gene acts as an internal standard and it does not display any changes in the expression level.

The proteins such as cytochrome c, caspases -9 and caspases -3 showed the enhanced expression with time-dependent manner (Fig. 5). The percentage of protein expression level was increased when accelerating the time of AgNPs treatment when compared with control A549 cells. The caspase -3 expression profile displayed up-regulated in the biogenic AgNPs treated A549 cells. From this examination, it is proven that the up-regulation of cytochrome c and caspase 9 triggered the level of caspase 3 activations. Caspase -3 is a key effector caspase and is activated through either the death-receptor or mitochondria-mediated pathway [30]. It has also been reported that apoptosis mediated by p53 induced the membrane translocation of Bax and cytosolic release of cytochrome c, which might amplify the apoptotic signal by activating caspase -9 and other downstream caspases like caspases -3, -6, and -7 [31]. Cytochrome c act as a necessary factor for the creation of ATP also plays a central role in apoptosis. The mechanism behind the activation of the cascade by the release of mitochondrial cytochrome c (mtCyt c) results active caspase-3 subsequently cleaves a variety of substrates resulting in characteristic morphologic changes in the nucleus, DNA fragmentation, and appearance of the phagocytic marker phosphatidylserine on the cell surface [32]. Taken together, our present findings clearly demonstrated the underlying mechanisms and principal mode of cell death induced by AgNPs was intrinsic mitochondrial-mediated apoptosis pathway in A549 cells.

3.6. Histopathological study

The toxicity effect of AgNPs to the living system is carefully investigated by *in vivo* analysis. For this study, we used Hematoxylin and Eosin stains of tissues from mice that were treated with cotton plant-mediated AgNPs. Interestingly, there is no pathological clue were discovered in the AgNPs treated mice group, it showed that AgNPs have not caused any toxicity to major organs. Collectively, we further conclude that there are no changes detected between major organs of AgNPs treated and saline control group as depicted in Figs. 6 and 7. No pathological lesions were identified in the silver nanoparticles (*Cleistanthus collinus*) treated group that could be indicative of toxicity [6]. The AgNPs measuring range of 4 nm were found to generate much higher levels of reactive oxygen species (ROS) production and interleukin-8 secretion from macrophage immune cells than 20 and 70 nm AgNPs [33], revealing that the sizes of the particles may attribute the principal factor affecting the toxicity of AgNPs. There are various methods are discovered for AgNPs synthesis, among them biological methods are simple, rapid, non-toxic, reliable, and green approaches using plant extracts which can make well-defined size and morphology under optimized conditions for translational research [37]. In the end, a green chemistry approach for the synthesis of AgNPs shows much promise. Apparently, the exposure time to nanoparticles, their concentrations, routes of applications and particle sizes of silver ions can all play a role, either singly or in concert, in AgNPs behavior and toxicity [34]. Several studies suggest that silver ion dissolution from AgNPs is dependent on particle size, with smaller AgNPs exhibiting higher dissolution because of their higher surface area-to-volume ratio [35,36]. Due to tremendous utilization of nano-materials, related products may led to bioaccumulation of AgNPs in the major tissues of living organisms subsequent various illness conditions, hence the toxic quality of nanomaterials must be cautiously evaluated. The present

study suggests that the industrially beneficial plant cotton mediated AgNPs can be actively exploited for the therapeutic role against lung cancer disease.

4. Conclusion

In conclusion, the above-proposed research findings in human lung cancer cells provide evidence of the molecular events involved in the apoptosis cell death induced by biologically synthesized silver nanoparticles. Here, demonstrated the activation of the intrinsic apoptotic pathway in the cancer cell is related to the disruption of mitochondrial membrane stability by alterations in the expression of pro- and anti-apoptotic proteins. Finally, the loss of membrane potential would act as a channel to release the cyt c from mitochondria into the cytosol and activate caspases -9 and -3. Ultimately, the activated cleaved caspases are responsible for apoptosis mediated cell death by causing DNA damage and nuclear condensation. In the end, we confirmed that cotton plant-mediated AgNPs has the potential to trigger apoptotic mode of cancer cell death and also we proved as safe to use for the biomedical applications. Thus, our current investigation clearly evidenced the mechanism and mode of green synthesized silver nanoparticles induced intrinsic apoptosis in human lung carcinoma cells.

Conflicts of interest

We wish to confirm that there are no known conflicts of interest associated with this publication and there has been no significant financial support for this work that could have influenced its outcome.

Appendix A. Supplementary data

Supplementary material related to this article can be found, in the online version, at doi:https://doi.org/10.1016/j.btre.2019.e00339.

References

[1] P. Rychahou, Y. Bae, D. Reichel, Y.Y. Zaytseva, E.Y. Lee, D. Napier, H.L. Weiss, N. Roller, H. Frohman, L. Anh-Thu, B. Mark Evers, Colorectal cancer lung metastasis treatment with polymer–drug nanoparticles, J. Control. Release 275 (2018) 85–91.

[2] R. Vivek, R. Thangam, S. Rajesh kumar, C. Rejeeth, G. Senthil Kumar, S. Sivasubramanian, S. Vincent, D. Gopi, S. Kannan, Multifunctional magnetite polymer therapeutic nanocomposites with "Off/On" mechanism for efficient and selective HER2 targeted Cancer therapy, Appl. Mater. Interf. 8 (2016) 2262–2267.

[3] Y. Li, Y. Wu, B.S. Ong, Facile synthesis of silver nanoparticles useful for fabrication of high-conductivity elements for printed electronics, J. Am. Chem. Soc. 127 (2005) 3266–3267.

[4] D.D. Evanoff Jr., G. Chumanov, Synthesis and optical properties of silver nanoparticles and arrays, Chem. Phys. Chem. 6 (2005) 1221–1231.

[5] K. Gunaseelan, K. Balaji, N. Kanipandian, K.S. Rajkumar, V. Nilmini, R. Thirumurugan, Biogenic synthesis and spectroscopic characterization of silver nanoparticles using leaf extract of *Indoneesiella echioides*: *in vitro* assessment on antioxidant, antimicrobial and cytotoxicity potential, Appl. Nanosci. 6 (2016) 973–982.

[6] N. Kanipandian, S. Kannan, R. Ramesh, P. Subramanian, R. Thirumurugan, Characterization, antioxidant and cytotoxicity evaluation of green synthesized silver nanoparticles using *Cleistanthus collinus* extract as surface modifier, Mater. Res. Bull. 49 (2014) 494–502.

[7] A. Jemal, F. Bray, M.M. Center, J. Ferlay, E. Ward, D. Forman, Global Cancer statistics, CA Cancer J. Clin. 61 (2011) 69–90.

[8] F.R. Khuri, R.S. Herbst, F.V. Fossells, Emerging therapies in nonsmall-cell lung cancer, Ann. Oncol. 12 (2001) 739–744.

[9] A. Jemal, R. Siegel, E. Ward, Y. Hao, J. Xu, T. Murray, M.J. Thun, Cancer statistics 2008, CA Cancer J. Clin. 58 (2008) 71–96.

[10] A. Das, J. Bortner, D. Desai, S. Amin, K. El-Bayoumy, The selenium analog of the chemopreventive compound S,S'-(1,4-phenylenebis[1,2-ethanediyl]) bisisothiourea is a remarkable inducer of apoptosis and inhibitor of cell growth in human non-small cell lung cancer, Chemico-Biol. Interact. 180 (2009) 158–164.

[11] J.N. Jenkins, Cotton, Traditional Crop Breeding Practices: an Historical Review to Serve As a Baseline for Assessing the Role of Modern Biotechnology, OECD, 2003, pp. 61–70.

[12] C.L. Brubaker, F.M. Bourland, J.E. Wendal, The origin and domestication of cotton Chapter 1.1., in: C.W. Smith, J.T. Cothern (Eds.), Cotton: Origin, History, Technology and Production, John Willey and Sons Inc, New York, 1999, pp. 3–33.

[13] N. Kanipandian, R. Thirumurugan, A feasible approach to phyto-mediated synthesis of silver nanoparticles using industrial crop *Gossypium hirsutum* (cotton) extract as stabilizing agent and assessment of its *in vitro* biomedical potential, Indus. Crops Prod. 55 (2014) 1–10.

[14] V. Sharma, D. Anderson, A. Dhawan, Zinc oxide nanoparticles induce oxidative DNA damage and ROS-triggered mitochondria mediated apoptosis in human liver cells (HepG2), Apoptosis 17 (2012) 852–870.

[15] Z. Darzynkiewicz, X. Li, J. Gong, Assays of cell viability: discrimination of cells dying by apoptosis, Methods Cell Biol. 41 (1994) 15–38.

[16] S. Devari, S. Jaglan, M. Kumar, R. Deshidi, S. Guru, S. Bhushan, M. Kushwaha, A.P. Gupta, S.G. Gandhi, J.P. Sharma, S.C. Taneja, R.A. Vishwakarma, B. Ali Shah, Capsaicin production by *Alternaria alternata*, an endophytic fungus from *Capsicum annum*; LC–ESI–MS/MS analysis, Phytochemistry 98 (2014) 183–189.

[17] R. Thangam, M. Sathuvan, A. Poongodi, V. Suresh, K. Pazhanichamy, S. Sivasubramanian, N. Kanipandian, G. Nalini, R. Rengasamy, R. Thirumurugan, S. Kannan, Activation of intrinsic apoptotic signaling pathway in cancer cells by *Cymbopogon citratus* polysaccharide fractions, Carbohydr. Polym. 107 (2014) 138–150.

[18] M. Jeyaraj, M. Rajesh, R. Arun, D. Mubarak Ali, G. Sathishkumar, G. Sivanandhan, G. Kapildev, M. Manickavasagam, K. Premkumar, N. Thajuddin, A. Ganapathi, An investigation on the cytotoxicity and caspase-mediated apoptotic effect of biologically synthesized silver nanoparticles using *Podophyllum hexandrum* on human cervical carcinoma cells, Colloids Surf. B Biointerfaces 102 (2013) 708–717.

[19] X. Zhang, F.L. Kiechle, HOECHST 33342 induces apoptosis and alters tata Box binding protein/DNA complexes in nuclei from BC3H-1 myocytes, Biochem. Biophys. Res. Commun. 248 (1998) 18–21.

[20] M.A. Siddiqui, H.A. Alhadlaq, J. Ahmad, A.A. AlKhedhairy, J. Musarrat, M. Ahamed, Copper oxide nanoparticles induced mitochondria mediated apoptosis in human hepatocarcinoma cells, PLoS One 8 (2013)e69534, doi: http://dx.doi.org/10.1371/journal.pone.0069534.

[21] H.M. McBride, M. Neuspiel, S. Wasiak, Mitochondria: more than just a powerhouse, Curr. Biol. 16 (2006) 551–560.

[22] T. Nakazato, K. Ito, Y. Ikeda, M. Kizaki, Green tea component, catechin, induces apoptosis of human malignant B cells via production of reactive oxygen species, Clin. Cancer Res. 11 (2005) 6040–6049.

[23] R.J. Youle, A. Strasser, The BCL-2 protein family: opposing activities that mediate cell death, Nat. Rev. Mol. Cell Biol. 9 (2008) 47–59.

[24] V. Gogvadze, S. Orrenius, B. Zhivotovsky, Multiple pathways of cytochrome c release from mitochondria in apoptosis, Biochim. Biophys. Acta 1757 (2006) 639–647.

[25] H. Wu, H. Zhu, X. Li, Z. Liu, W. Zheng, T. Chen, B. Yu, K.H. Wong, Induction of apoptosis and cell cycle arrest in A549 human lung adenocarcinoma cells by surface-capping selenium nanoparticles: an effect enhanced by polysaccharide−Protein complexes from Polyporus rhinoceros, J. Agric. Food Chem. 61 (2013) 9859–9866.

[26] V. Jendrossek, Targeting apoptosis pathways by Celecoxib in cancer, Cancer Lett. 332 (2013) 313–324.

[27] C. Jiang, Y.F. Yang, S.H. Cheng, Fas ligand gene therapy for vascular intimal hyperplasia, Curr. Gene Ther. 4 (2004) 33–39.

[28] S.I. Han, Y.S. Kim, T.H. Kim, Role of apoptotic and necrotic cell death under physiologic conditions, BMB Reprod. 41 (2008) 1–10.

[29] H. Henry, A. Thomas, Y. Shen, E. White, Regulation of the mitochondrial checkpoint in p53-mediated apoptosis confers resistance to cell death, Oncogene 21 (2002) 748–760.

[30] C. Huang, X. Chen, B. Guo, W. Huang, T. Shen, X. Sun, P. Xiao, Q. Zhou, Induction of apoptosis by icariside II through extrinsic and intrinsic signaling pathways in human breast cancer mcf7 cells, Biosci. Biotechnol. Biochem. 76 (2012) 1322–1328.

[31] C.F. Gao, S. Ren, L. Zhang, T. Nakajima, S. Ichinose, T. Hara, K. Koike, N. Tsuchida, Caspase-dependent cytosolic release of cytochrome c and membrane translocation of Bax in p53-induced apoptosis, Exp. Cell Res. Suppl. 265 (2001) 145–151.

[32] J. Cai, J. Yang, D.P. Jones, Mitochondrial control of apoptosis: the role of cytochrome c, Biochim. Biophys. Acta 1366 (1998) 139–149.

[33] J. Park, D.H. Lim, H.J. Lim, T. Kwon, J.S. Choi, S. Jeong, I.H. Choi, J. Cheon, Size dependent macrophage responses and toxicological effects of Ag nanoparticles, Chem. Commun. (Camb.) 47 (2011) 4382–4384.

[34] M.B. Genter, N.C. Newman, H.G. Shertzer, S.F. Ali, B. Bolon, Distribution and systemic effects of intranasally administered 25 nm silver nanoparticles in adult mice, Toxicol. Pathol. 40 (2012) 1004–1013.

[35] R. Ma, C. Levard, S.M. Marinakos, Y. Cheng, J. Liu, F.M. Michel, G.E. Brown, G.V. Lowry, Size-controlled dissolution of organic-coated silver nanoparticles, Environ. Sci. Technol. 46 (2) (2012) 752–759.

[36] Z.M. Xiu, Q.B. Zhang, H.L. Puppala, V.L. Colvin, P.J. Alvarez, Negligible particle-specific antibacterial activity of silver nanoparticles, Nano Lett. 12 (2012) 4271–4275.

[37] X.F. Zhang, X.G. Liu, W. Shen, S. Gurunathan, Silver nanoparticles: synthesis, characterization, properties, applications, and therapeutic approaches, Int. J. Mol. Sci. 17 (2016) 1534.